

PROCEEDINGS REPRINT

 SPIE—The International Society for Optical Engineering

Reprinted from

Sensors and Sensor Systems for Guidance and Navigation II

22-23 April 1992
Orlando, Florida



Volume 1694

Scanning laser aircraft surveillance system for carrier flight operations
AA. Vetter, D.M. Shemwell, R.I. Gellert, and J. Black

Humbug Mountain Research Laboratories
P.O. Box 1380, Duarte, CA 91009

ABSTRACT

The Scanning Laser Aircraft Surveillance System (SLASS) uses two scanning infrared laser beams to illuminate retroreflectors located on aircraft landing gears and hook to determine very precisely the azimuthal, ascension, yaw, roll, and pitch angles of the aircraft in the approach corridor. The range, approach velocity, and aircraft type are also determined. Aircraft configuration is determined by the presence or absence of each return signal, and aircraft type is identified with an encoded sequence of retroreflectors on one landing gear. The position of the aircraft is determined by the time in the scan that the beam encounters the retroreflectors.

2. IDENTIFICATION OF THE PROBLEM

If better information were presented to the Landing Signal Officer (LSO), the Carrier Air Traffic Control Center (CATCC), and the Air Boss a reduction in landing mishaps and missed approaches to an aircraft carrier may be achieved. During periods where optical visibility of the carrier approaching aircraft is limited, such as during night operations or in adverse weather, there can be difficulty in identifying the exact location, aircraft type, and aircraft configuration. The LSO needs to identify the type of approaching aircraft so that he can determine if it is approaching within the permitted envelope for that particular aircraft. The aircraft type and weight, determined from the descent rate and airspeed, needs to be identified so that the pressure on the damping cylinders attached to the arresting cable can be set.

3. PRINCIPLES OF OPERATION

The SLASS operates by having two scanning infrared laser beams sweep out the approach corridor from below the ramp of the carrier. As illustrated in Figure 1, one laser beam is wide in the ascension direction and swept in the azimuthal direction, and the other beam is wide in the azimuthal direction and is swept in the ascension direction. Retroreflectors placed on the landing gear and hook of the aircraft are used to return a signal to a receiver located adjacent to the transmitting station. Temporal resolution of the return signals provides data on the six degrees of freedom (range, ascension, azimuth, yaw, pitch, and roll). Successive sweeps are used to determine the rate of approach and rates of change in glideslope and line-up. A separate series of retroreflectors placed vertically on one landing gear provides identification of the aircraft type.

The scan rate is much slower than the time required for the light to travel round trip to the approaching aircraft. Consequently, the angle of the aircraft in the ascension direction is determined by the location of the ascension scanning beam when the return is received. Similarly, the time at which the signal from the azimuthally scanned beam arrives determines the azimuthal position of the aircraft.

The series of identification retroreflectors placed on one of the landing gear are aligned vertically as illustrated in Figure 2. As the ascension scanning beam (illustrated to the left side) passes successively over the retroreflectors, the amount of light returned to the detector is varied according to the size of the retroreflector. Two different sizes are chosen so that the intensity of the return from the larger retroreflector is twice that from the

smaller retroreflector. With two sizes of retroreflectors, the return signal is modulated into a two level data word with each retroreflector corresponding to a data bit. Note that since this is a two level system, the absolute intensity is not important, just the relative intensity, and each bit provides a positive signal (no signal is ambiguous). A four bit data word would provide a total of 16 different aircraft types which could be identified.

By placing one retroreflector on each of the three landing gears and the hook, data on six degrees of freedom can be obtained. Two retroreflector sizes are utilized to differentiate the source of the signals; the larger retroreflector will have a higher amplitude return. As shown in Figure 3, the return from the azimuthal scan provides data on the azimuthal position, yaw, and range. Once the type of aircraft has been identified, then the distance between the landing gears is known, and the range is then determined from the time taken for the laser beam to sweep from one main landing gear to the other and sweep rate. The yaw angle is determined from the difference between the sweep time from hook retroreflector to the nose gear retroreflector. Note that the absolute intensity of the return signals is not important. The determination of the position depends upon temporal resolution of the return signal from the scanning beams, not spatial resolution of the return beam.

As illustrated schematically in Figure 3, the return signal from the ascension scan provides information from which the ascension, pitch, and roll angles can be determined. The difference between the two returns from the main landing gears indicates the degree of roll, and the difference between the returns from the nose gear and the hook yields the pitch angle.

The aircraft configuration is easily determined from the SLASS signal. If a return signal is acquired, then the corresponding appendage is known to be down. From Figure 3, it can be seen that the return signal from the nose gear is distinguished from that from the main landing gears by its intensity and location in the sequence.

4. ANALYSIS

The concept of the SLASS is straight forward, but implementation of functional hardware presents the optical designer with some interesting choices. The optical system provides for the SLASS functions of beam shaping, scanning, projection, and collection. The values of the parameters and sizes for a design are listed in Table 1. The complete system requires two such units; one to scan the azimuth and one to scan in ascension.

The design incorporates a xenon-helium laser operating at a wavelength of 3508 nm with an output power of 120 mW. The main reasons for the choice of this type laser are the adequate power level, coincidence with an atmospheric transmission window, and fog penetration capability. A middle infrared laser is also chosen so that the beams are not visible to the pilot, hence add no distraction to the view on approach. Light with this wavelength is considered "eye-safe" and will protect the pilot from ocular damage [1]. This wavelength is also the transmission cutoff for most glasses and plastics (such as aircraft canopies) [2], so that the laser beam is absorbed before it reaches the pilot.

The optical design chosen is shown in Figure 4. It incorporates several interesting features. From the laser, the light is routed through a series of beam shaping optics. These optics serve two purposes: to expand the beam to an appropriate projection size (i.e. 100 mm at the exit aperture), and to impress upon the beam a divergence of approximately 5°. The cylindrical lens is located at the first focal point in the diagram. By placing the cylindrical lens near the focus it is easy to adjust the divergence to the desired value. The primary objective lens in the beam shaping optics is located just prior to the scan mirror. This lens produces a large, but converging beam. When this beam intercepts the scan mirror its normal area is a 50 mm diameter circle. The beam comes to a focus after it leaves the scan mirror. Expanding from this focus it arrives at a collimation lens and by now it has expanded to its full 100 mm diameter size. This lens collimates one axis while the other axis

will continue to expand at approximately 5° . In addition to collimating, this lens images the scanning mirror onto the fold mirror which serves as the exit aperture. The scan mirror is moved to form the sweeping action of the SLASS system. In this case, the fold mirror exit aperture, scanning mirror, and collimating lenses are located so as to place the fold mirror in an image plane of the scanning mirror. By using a non-unity imaging relationship, such as the 2:1 ratio shown in the schematic diagram, the size of the scanning mirror is reduced. The end result of the transmitter portion is a cylindrically expanding beam which appears to emerge from the final fold mirror while executing a scan.

The azimuthal and ascension scans alternate with a full cycle rate of 15 Hz. At a relative approach speed of 110 knots (140 knot airspeed and a 30 knot wind over deck) the distance that the aircraft travels in a scan cycle is 3.8 m (12 feet).

The field of view for the design is 4° in ascension and 5° in azimuth. The design values for the ascension angular scan rate, s_u , and azimuthal angular scan rate, s_v , are 2.1 and 2.6 rad/s, respectively.

The final fold mirror provides a 100 mm beam which at the output plane is converging in the direction of scan and diverging in the direction perpendicular to the scan. The laser beam impinges 14 optical surfaces in the transmitting optics. Assuming that the reflective and scatter loss is 1% per surface, then the efficiency of the transmitting optics, E_p , is 0.87. For the design case, the peak irradiance at the exit aperture is less than 1 mW/cm^2 , a factor of 100 below the MPE (maximum permissible exposure) for direct ocular exposure [3].

In the direction of the scan, the beam is focused at a distance of 2 nmi. In the direction perpendicular to the scan direction, the beam is constantly expanding. Since illumination is not desirable outside of the FOV, the beam will be vignetted in the direction perpendicular to the scan direction. Using a Gaussian beam shape, the fraction of laser power in the FOV is 0.82.

The effect of turbulence on the SLASS beam is approximated by an increase in the beam radius [4,5]. Intermediate turbulence ($C_N = 8 \times 10^{-9} \text{ m}_{-1/3}$ [6]) has a small effect on the beam waist; at a range of 2 nmi, it increases the beam waist 1%, from 103 to 104 mm. Strong turbulence ($C_N = 5 \times 10^{-7} \text{ m}_{-1/3}$ [6]) increases the beam waist significantly at long range; at a range of 2 nmi, the beam waist increases from 103 to 225 mm.

The most powerful line of the xenon-helium laser line at 3508 nm has a transmission of approximately 0.725 over a 10 km path; this is equivalent to an extinction coefficient of $3.2 \times 10^{-2} \text{ km}^{-1}$ [7].

The scattering term is dominated by particle (Mie) scattering [8]. The Xe-He laser, has outstanding characteristics for penetration of haze. The attenuation at this wavelength when visible light has a 3 mile visibility (VFR limit) is the same as for visible light in a standard clear atmosphere [7]. The extinction coefficient and scattering transmission are given for the design in Table 1.

With the 3.5 micrometer wavelength xenon-helium laser, a 100 mm diffraction limited output beam from the, SLASS scanner will produce an approximately 100 mm diameter focused spot at 2 miles under ideal conditions. This yields an essentially constant diameter beam throughout the final 2 miles of the aircraft's approach. This diameter sets the maximum effective size of the retroreflectors, since the amount of return signal will not increase very much as the diameter increases beyond the spot size in the direction of scan. Therefore, a retroreflector size of 75 mm has been selected.

Rather than using a single 75 mm retroreflector, an array of smaller corner cubes is used. For the design, the retroreflector is composed of a multiple celled retroreflector arrays with each cell 10 mm in diameter. The individual small retroreflector will have a larger diffractive spread than a single large reflector; however, a small aperture can tolerate larger deviations from perfection before it reaches its diffraction limit. There are three major advantages of the multi-celled array over the single retroreflector. First, the depth of the retroreflector is roughly the same as its diameter. Consequently, a multi-celled array will require less volume and will weigh less. Second, the shape of the single cell retroreflector is round or hexagonal, while the outline of the multi-celled array can be shaped to fit the area available. Note also that the multi-celled retroreflector does not need to be flat, but can be shaped to follow contours of the supporting structure. This is particularly important since the retroreflector should be aligned with the SLASS on the nominal approach, which implies that the retroreflector should be aimed downwards at an angle equal to the nominal approach angle plus the aircraft angle of incidence. A single retroreflector would protrude outwards to accommodate this downward angle a distance roughly equal to the cell diameter times the sine of the downwards angle, while each cell of the array could be staggered so that the protruding distance would be decreased roughly as the ratio of cell size to array size. Third, the single cell reflects back a narrow beam which, due to either manufacturing tolerances or atmospheric steering, may miss the collector. The smaller cells have larger beam spread and the multitude of cells ensures that signal will always reach the receiver. There is another advantage from the design viewpoint: the cell size (which determines the spread of the return beam) and total cross sectional area (which determines the amount of light in the return beam) are independent. Consequently, the relative intensity of the return beams from different sized retroreflectors would be independent of range.

The relative amplitudes of the return pulses are shown in Figure 5. As the range increases from 0.1 to 1 nmi, the width of the return signal decreases because the beam waist remains approximately the same value while the time that the beam hits the retroreflector decreases inversely with range. Note that if the beam were expanding linearly with range, as it does in the direction perpendicular to the scan, then these two factors would cancel and the width of the return signal would be independent of range. At long range, the turbulence spread dominates and the width of the return signal increases with range. The temporal dependence of the signal for azimuthal scan the at 2 nmi is shown in Figure 6.

The retroreflectors have two different sizes. The larger size is 75 by 75 mm and the smaller size is 50 mm by 50 mm. The retroreflector cell size is chosen to be 10 mm for both the larger and smaller retroreflectors. The sizes are chosen so that the intensity of the return signal, which is proportional to the retroreflector area, is twice as large from the larger retroreflector than from the small one. Note that the absolute intensity is not important, just the relative intensity.

In order to provide an easily interpreted signal, the width of the laser beam in the scanning direction should be smaller than the distance between the retroreflectors. In practice, however, the resolvability of two adjacent point sources is less stringent. As noted previously, the beam waist is 104 mm with intermediate turbulence and 225 mm in strong turbulence. Thus, to ensure resolution at 2 nmi, the separation of the retroreflectors in the identification sequence would need to be 250 mm. The identification assembly would then need to be slightly longer than 0.75 in. The return from the identification sequence at a range of 2 nmi is shown in Figure 7 for intermediate turbulence and Figure 8 for strong turbulence. The identification sequence is seen to be near the resolution limit at 2 nmi in strong turbulence, but with intermediate turbulence the sequence is easily resolved.

Different sized retroreflectors can be used on the landing gear and hook to simplify the discrimination of the signals from each of the locations. For example, place the larger sized retroreflectors on the hook and right main gear, use both smaller and larger sized retroreflectors for the identification sequence on the nose gear, and

use a smaller sized retroreflector on the left main gear. The sequence of the resulting return signals is illustrated schematically in Figure 9.

The return signals from the left and right gears are readily distinguished as are the return signals from the hook and nose gear. Simple interpretation permits rapid data reduction for the positional angles and range.

The scanning motion of the SLASS beam across a retroreflector converts spatial information to temporal information. The bandwidths of the return signal are given as a function of range in Figure 10. At close range, the beam waist is nearly constant so that the bandwidth increases nearly linearly with range due to the shorter time that the scanning beam hits the retroreflector. At longer range, the beam waist increases so that the time that the scanning impinges on the retroreflector also increases. With strong turbulence, at long range the bandwidth decreases as $R^{3/5}$.

Each retroreflector cell can be considered an individual aperture for the return beam. Since the cell size is much smaller than the waist of the scanning beam, the return beam will be symmetric and will have the same divergence for each retroreflector for both azimuthal and ascension scanning beams. Diffractive spread dominates over the entire range of interest. A diameter of the collecting mirror has been chosen to be 0.69 m to match the diffractive spread of the corner cube cells and because it is a practical size, which is easily fabricated for use at the operating wavelength. With a retroreflector cell size of 10 mm and strong turbulence, the beam waist at the receiving mirror is 0.83 m at a range of 2 nmi, and the fraction of power captured by the receiving mirror is 0.28.

The light from the retroreflectors is directed back towards a collector onboard the carrier. The collecting aperture is located coaxially with the exit aperture of the transmitter. The primary mirror is combined with a lens to form a telescope, but because the target can be anywhere in the field of regard, a detector placed after these two optical elements would have the entire approach corridor in its field of view. To limit the field of the detector, a special set of receiving optics has been designed.

As the scan mirror sweeps the transmitted beam, the region covered by the SLASS beam is formed into a line image by the receiving telescope, and this potential line image also sweeps across its field of regard. The image of the field of illumination moves back and forth across the focal plane as the scan mirror moves. Light from this image plane is collimated by the secondary lens to produce a field-of-regard collimated in one axis which changes its tilt as the beam scans. The motion of the descan mirror is synchronized to the scan mirror so that it rotates to remove the changing tilt from the field-of-regard. The potential image of the SLASS scan at this point is a line which has lateral motion corresponding to the sweep of the scan mirror. This light is perpendicularly incident on a focusing lens which reduces the field-of-regard to a single image, effectively eliminating one dimension of the FOV needed by the detector. This line image is also an ideal position to place a baffle or aperture stop which ensures the reduced FOV. Note also that backscattered light from the near field, that is for close ranges not of interest for the SLASS, will not be in focus at the baffle, so that much of the backscattered light will be blocked from the detector. To further reduce the required size of the detector, an anamorphic telescope is used to collapse the line image along its long axis. With this optical train, the detector tracks the region of illumination. These collection optics finally concentrate the available return light onto a detector. A detector with an area of 4 mm² has been chosen. An optical bandpass filter is placed in front of the detector.

There are 13 optical surfaces that the beam reflects from or refracts through in the receiving optics. Estimating a 1% loss per surface for these 13 surfaces and a 50% transmittance of the laser line filter, the efficiency of the receiving optics, E_r , is taken to be 0.44. The peak power in the return pulse is shown in Figure 11 for

atmospheric conditions with a visual range of 5 km (VFR limit). Both the azimuthal and ascension scans are shown for both strong and intermediate turbulence. These power levels correspond to the center of the scanning beam. The power level is one-half this value at the extremities of the beam in the direction perpendicular to the scan.

A HgCdTe detector, cooled to 80 K, has been chosen because of its high detective properties and good frequency response [2]. With a signal bandwidth of 20 kHz, the noise equivalent power (NEP) of the detector is 2.6×10^{-10} W.

The signal-to-noise ratio (SNR) is given as a function of range in Figure 12. The SNR is shown for both the azimuthal and ascension scans and for both strong and intermediate turbulence levels with a 5 km visibility. At short range, the SNR actually increases with range due to the increase in collection efficiency. The maximum range is approximately 5 nmi. As shown in Figure 13, better performance is obtained at long range with standard clear visibility (visual range of 23.5 km). With a visibility of 0.5 nmi, SLASS still has adequate SNR beyond 2 nmi, as shown in Figure 14.

The bandwidth of the return signal varies from 1 to 20 kHz. When the SLASS beam scatters off of fog and other atmospheric aerosols, the time dependence of the received scattered light will correspond to the time required for the beam to scan over the obscuring structure. In addition, the scattered light is not retroreflected, but is diffuse. This means that its intensity will fall off with the square of its distance from the illuminator. Thus, only the fog and clouds that are relatively close to the carrier will contribute significant backscatter into the receiving telescope. These structures are both uniform and large when compared to the retroreflectors on the aircraft, which makes the frequency of these backscattered signals range all at low frequencies. Because the SLASS signals and the noise signals due to backscatter lie in different frequency realms, it will be possible to suppress the backscattered noise through the use of a high pass filter.

The backscatter is also optically discriminated. The backscatter from directly in front of the SLASS transmitter is blocked from the primary mirror by the center obscuring output mirror. Furthermore, the backscatter from the near field which illuminates the primary mirror is out of focus at the baffle; consequently, most of the backscatter which is collected by the primary mirror will not reach the detector.

5. UNCOUPLING THE SLASS SIGNALS

In order to understand the uncoupling of the SLASS signals, consider a slightly simplified system consisting of a single retroreflector on each of the nose landing gear, left main landing gear, right main landing gear, and the hook. Choose a coordinate system for the aircraft whose origin is defined by the longitudinal axis and the manufacturer's datum point. Let the x-axis coincide with the longitudinal axis and be positive towards the tail of the aircraft. Define the y-axis to be perpendicular to the longitudinal axis and parallel to the wings with the positive side corresponding to the right wing. The z-axis is then in the vertical direction defined by the right-hand rule.

The aircraft roll, pitch, and yaw angles as measured by the SLASS are defined relative to the direction to the point of origin of the SLASS. Let the roll angle, a_r , be a clockwise rotation about the x-axis. Thus, a positive roll angle lowers the right wing and raises the left wing. With a roll angle of zero, the z-axis is perpendicular to the direction from the laser transmitter in the vertical direction. Let the yaw angle, a_y , be a clockwise rotation about the z-axis. Thus, a positive yaw angle places the nose towards the right. With a yaw angle of zero the aircraft is aimed directly at the laser transmitter. Let the pitch angle, a_p , be a clockwise rotation about the y-

axis. Thus, a positive pitch places the nose upwards. With a zero pitch angle, the x-axis is colinear with the beam from the transmitter, not level.

Define t_v as the time for the scan to progress from the center of a retroreflector to the origin of the coordinate systems. Since only relative times are used to determine the position angles and range, any reference point could have been chosen, but the use of the coordinate system origin simplifies the mathematics; the final equations will be independent of the reference location. Assume that the ascension scan is upwards from the horizontal. Then,

$$R \sin s_v t_v = \begin{aligned} & x (-\sin a_p \cos a_y + \cos a_p \sin a_r \sin a_y) \\ & + y (-\sin a_p \sin a_y - \cos a_p \sin a_r \cos a_y) \\ & + z (\cos a_p \cos a_r) \end{aligned} \quad (1)$$

where R is the range from the transmitter to the aircraft and s_v is the angular rate of scan of the ascension scanning beam. Similarly, define t_u as the time difference for the azimuthal scan with the beam scanning from (pilot's) left to right across the aircraft. Then

$$R \sin s_u t_u = x (-\sin a_y \cos a_r) + y (\cos a_r \cos a_y) + z \sin a_r$$

where s_u is the angular rate of scan of the azimuthal scanning beam.

Use the subscripts h, n, l, and r to correspond to the return from the retroreflectors on the hook, nose landing gear, left main landing gear, and right main landing gear, respectively. Once the aircraft has been identified, then the x, y, and z values for the locations of each of the retroreflectors would be known. Consider the sequence of return signals as illustrated in Figure 3. The multiple signals in the identification sequence pose no difficulty in determining the time mark as either the first or last one (or even mid point) in the sequence can be utilized. There are four signals for each direction of scan from which three time differences can be determined. Thus, there are 6 measured quantities (4 independent) to determine the three positional angles and the range.

The following simplifications are useful to understand how the aircraft position and range are best determined: $y_n = 0$; $y_h = 0$; $x_r = x_l$; $y_r = -y_l$; $z_r = z_l$; and $z_r = z_l = z_n = z_h$. Furthermore, consider the case where the position angles are small and expand them to first order so that the cosines are nearly 1 and the sines are nearly equal to their argument. The result is

$$R = (y_r - y_l) / s_u (t_{u,r} - t_{u,l}) \quad (3)$$

$$a_y = R s_u (t_{u,n} - t_{u,h}) / (x_h - x_n) \quad (4)$$

$$a_p = r s_v (t_{v,n} - t_{v,h}) / (x_h - x_n) \quad (5)$$

$$a_r = r s_v (t_{v,r} - t_{v,l}) / (y_r - y_l) \quad (6)$$

Thus, the range and yaw angle are best determined from the azimuthal scan and the pitch and roll angles are best determined from the ascension scan.

For either physical or tactical reasons, a retroreflector may not be able to be placed on the hook. Then the SLASS would not be able to determine if the hook is down. However, the pitch and yaw angles can still be determined from the other signals with only one additional step. The pitch angle is determined from the difference between the returns from the nose gear and the mean of the returns from the main gear on the ascension scan. The yaw angle is determined from the difference between the differences in the returns from

the right main gear and the nose gear and the nose gear and the left main gear on the azimuthal scan.

The data reduction for the SLASS determines the position angles and range in relation to the SLASS beam. However, the best location for the transmitter and receiver is below the rounddown at the stern of the carrier. This location leads to a difference between the measured positional angles and range and the actual values with respect to the proper approach. These corrections are determined from geometrical considerations.

A functional diagram of the signal processing for the SLASS is given in Figure 15. The raw data from the ascension scanner is fed into a dedicated processor and directly to the main processor. This dedicated processor interprets the signal to verify that the nose gear and hook are down, identify the aircraft type, and generates roll and pitch data. The raw data from the azimuthal scanner is also fed into a dedicated processor and directly to the main processor. This dedicated processor interprets the signal to verify that both main gear are extended and generates range and yaw data. The two dedicated processors exchange data as interpretation of the range and yaw data require knowledge of the physical separation of the retroreflectors which is dependent on the aircraft type. Second order corrections, e.g. pitch and roll corrections for the range and yaw calculations, are also made by the dedicated processors with the exchanged data. The main processor accepts all of the inputs, reduces the data to a useful form, maintains a record of the approach path, calculates the rates of change, makes comparisons with the acceptable limits for the particular aircraft type, generates graphical interpretations of the aircraft conditions, and outputs the data to displays for the LSO, CATCC, and Air Boss.

In actual implementation, the uncoupling equations are cast in terms of R , $\sin a_y$, $\sin a_p$, and $\sin a_r$:

$$R = (- (x_r - x_l \sin a_y \cos a_r + (y_r - y_l) \cos a_r \cos a_y + (z_r - z_l) \sin a_r) / \sin s_u (t_{u,r} - t_{u,l}) \quad (7)$$

$$\sin a_y = ((y_n - y_h) \cos a_r \cos a_y + (z_n - z_h) \sin a_r - R \sin s_u (t_{u,n} - t_{u,h})) / (x_n - x_h) \cos a_r \quad (8)$$

$$\sin a_p = (- R \sin s_v (t_{v,n} - t_{v,h}) + (x_n - x_h) \cos a_p \sin a_r \sin a_y - (y_n - y_h) \cos a_p \sin a_r \cos a_y + (z_n - z_h) \cos a_p \cos a_r) / ((x_n - x_h) \cos a_y + (y_n - y_h) \sin a_y) \quad (9)$$

$$\sin a_r = (- R \sin s_v (t_{v,r} - t_{v,l}) - (x_r - x_l) \sin a_p \cos a_y - (y_r - y_l) \sin a_p \sin a_y + (z_r - z_l) \cos a_p \cos a_r) / ((y_r - y_l) \cos a_p \cos a_y - (x_r - x_l) \cos a_p \sin a_y) \quad (10)$$

These equations would be solved numerically by using the updated signal data and the previous values for the remaining sine and cosine functions. Iteration is required to converge to the actual values.

The primary purpose of SLASS is to assist in the safe recovery of aircraft. To this end, it is essential that the information derived by SLASS be presented in a useful fashion to the LSO. The critical pieces of information derived by the SLASS are: position in the corridor, aircraft type, gear and hook down, range, airspeed, and angle of attack.

6. CONCLUSIONS

The Scanning Laser Aircraft Surveillance System (SLASS) was found to be able to determine the position, attitude, configuration, and type of an approaching aircraft. In clear weather, these functions can be performed at ranges beyond 5 nmi with a system which emits 0.2 W of infrared power into the approach corridor. In adverse weather the range of the system is diminished, but the SLASS would still provide effective data over the critical portions of the approach. A design of a SLASS for carrier flight operations has been developed using a xenon-helium laser operating at a wavelength of 3508 nm.

The ascension and azimuthal positions in the corridor, which can be interpreted as glideslope and line-up, are most readily determined by the SLASS. This information is available so long as a retroreflector signal is detectable. Analysis has shown that the range for detection of a single signal is greater than 4 nmi with a visibility of 5 km (VFR limit). However, for the ascension and azimuthal positional data, the individual returns do not need to be resolved. Therefore, the actual useful range for ascension and azimuth information is extended as the lack of optical resolution of the retroreflectors (particularly those used in the identification sequence) by the SLASS beams means that the return signal has a higher amplitude than from a single retroreflector and this combination signal is detectable at even longer ranges; with a visibility of 5 km, the useful range is extended approximately 1 nmi to 5 nmi. Because of the narrow width of the SLASS beam and the small size of the retroreflector, the angular resolution of the azimuthal and ascension position is very high. For example, at a range of 2 nmi these positions are determined to 1.1 arcseconds. Note that the positional resolution is a function of the SLASS beam width and is independent of the attenuation due to aerosols, so that it does not change due to adverse weather (so long as the signals are detectable).

The attitude of the approaching aircraft is determined by differences between the times of the return signals from the retroreflectors. The pitch is determined from the time difference between the signals from the nose gear and the hook during the ascension scan; the roll from the time difference between the signals from the right and left main gears during the azimuthal scan; and the yaw from the time difference between the signals from the nose gear and the hook during the azimuthal scan. The accuracy and precision of these data depend upon both the SLASS beam width and the angular separation of the retroreflectors on the gears and hook. The resolution of the SLASS decreases rapidly with distance, as R^{-1} at near ranges and R^{-5} at ranges where diffractive spreading dominates. However, over the ranges of interest, the SLASS provides resolution exceeding that required from a practical viewpoint. At a range of 2 nmi, the resolution of the pitch angle is 0.1° , roll angle 0.3° , and yaw angle 0.1° . Since the resolution of the SLASS beam is the limiting factor (so long as the signal significantly exceeds the noise), the range for acquisition of attitude information does not change due to adverse weather.

The configuration of the aircraft is determined by the presence of the return signals. The nose gear and hook are discerned from the ascension scan, and the right and left main gears are distinguished in the azimuthal scan. Since the separation of the retroreflectors on the aircraft (as projected into the plane perpendicular to the SLASS beam) is greater than the beam width at all ranges under consideration, the individual extensions can be identified whenever a single SLASS signal is detectable. Thus, the range for configuration identification varies with visibility conditions: from 5 nmi in a clear atmosphere; to 4 nmi in hazy (5 km visibility) conditions; to 2.3 nmi with 0.5 nmi visibility; to 1 nmi with 0.13 nmi visibility.

The aircraft type identification is determined by interpretation of the return signal from a series of four closely spaced retroreflectors which could be located on any one of the gears or the hook. The retroreflectors in the sequence has two different sizes so that when the SLASS beam is swept across the sequence, the return signal is modulated into a two level data word. Each aircraft type would be represented by a unique sequence. Once the aircraft type is known, then the distances between the gears and hook, which are required for reduction of the position and range data, are known. The range for aircraft type identification is determined by resolution of retroreflectors by the SLASS beam. For a retroreflector separation of 0.25 m (thus total assembly length of 0.8 m), the range for type identification is greater than 2 nmi. For this spacing, the worst case beam spread was assumed. Using the lower limit on beam spread, the spacing would be reduced to 0.1 m and the assembly length would be 0.4 m. Since the resolution of the SLASS beam is the limiting factor, the range for type identification does not change due to adverse weather, so long as the return signals are detectable.

The range is determined from the time difference between the signals from the right and left main gears during the azimuthal scan. The farthest distance for range information is the same as for the positional data. The SLASS does not determine range precisely, except at short ranges; at a range of 2 nmi, the resolution is 170 m.

7. ACKNOWLEDGMENTS

This work was supported by the U.S. Navy through the Small Business Innovation Research Program.

8. REFERENCES

- [1] D. Sliney and M. Wolbarsht, *Safety with Lasers and Other Optical Sources*, Plenum, 1980.
- [2] W.L. Wolfe and G.J. Wisis (ed.), *The Infrared Handbook*, Office of Naval Research, (revised edition) 1985.
- [3] American National Standards Institute, "American National Standard for the Safe Use of Lasers", ANSI Z136.1-1980, 1981.
- [4] H. Weichel, "Atmospheric Propagation of Laser Beams", *Proc. SPIE*, v. 547, pp. 1-15, 1985.
- [5] F.G. Gebhardt, "High Power Laser Propagation", *Applied Optics*, vol. 15, pp. 1479-1493, 1976.
- [6] M. Bertolotti, "Propagation Problems Relative to Laser Transmission", AGARD-CP-183, pp. 3-1 to 3-29, 1975.
- [7] R.A. McClatchey and J.E.A. Selby, "Atmospheric Attenuation of Laser Radiation from 0.76 to 31.25 μm ", AFCRL-TR-74-0003, 1974.
- [8] R.M. Measures, *Laser Remote Sensing*, Wiley, 1984.

Table 1. List of SLASS Design Parameters

Laser Type	Xe-He
Laser Wavelength	3508 nm
Laser Power	120 mW
Beam Quality	1.25
Transmitting Optics Efficiency	0.71 (includes vignetting)
Exit Aperture	100 mm
Focal Distance	2 nmi
Scan Field	4. ascension, 5. azimuth
Scanning Frequency	30 Hz
Scanning Angular Velocity	2.1 rad/s ascension, 2.6 azimuth
Power at Extremities of Wide Dimension	1/2 power at center
Retroreflector Total Size	75 by 75 mm square
Retroreflector Cell Size	10 mm
Retroreflector Effective Area Factor	0.9
Collecting Optic Size	0.69 m diameter
Receiver Optics Efficiency	0.44
Detector Type	HgCdTe (x=0.39, 80 K)
Detector D*	$1.1 \times 10^{11} \text{ cm Hz}^{-1/2} \text{ W}^{-1}$
Detector Area	4 mm^2
Bandwidth of Detector Circuit	20 kHz
Detector NEP	$2.6 \times 10^{-10} \text{ W}$
At Range of 2 nmi	
Transmission (Molecular Absorption)	0.89 (ga = 0.032/km)
Scattering Transmission (5 km visibility)	0.69 (gs = 0.10/km)
Turbulence Coefficient (intermediate)	$4 \times 10^{-8} \text{ m}^{-1/3}$
Wide Beam Gaussian Waist (5')	270 m
Narrow Beam Gaussian Waist	0.10 m
Laser Intensity at Retroreflector	4 mW/m^2 in center
Return Pulse (e-1) Width	30 us
Fraction of Return Signal Collected	0.29
Peak Power in Return Pulse	250 nW
Signal-to-Noise Ratio	1000

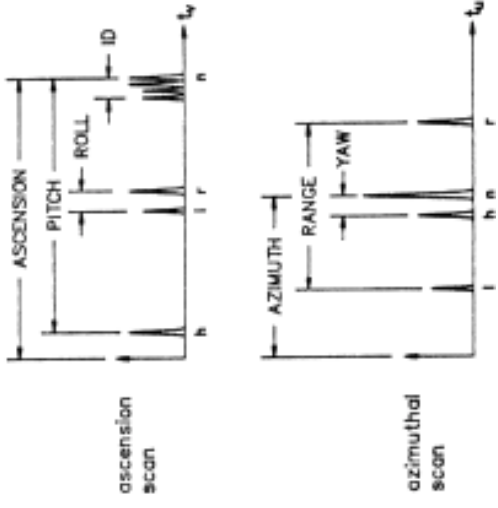


Fig. 3 Representation of the returns from SLASS scans. The signals used to determine the ascension, roll, and pitch angles from the ascension scan are on top, and the signals used to determine the azimuthal angle, yaw, and range from the azimuthal scan are on the bottom.

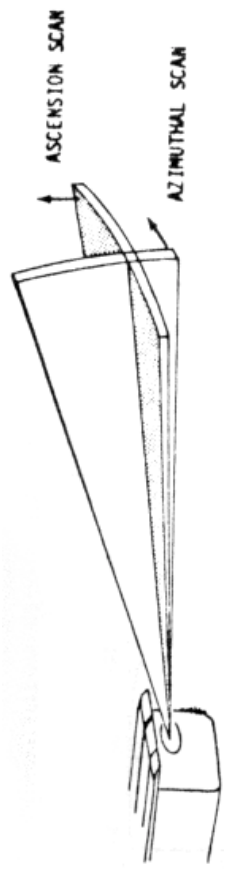


Fig. 1 Schematic of the azimuthal and ascension scanning laser beams of the SLASS from the stern of the aircraft carrier.

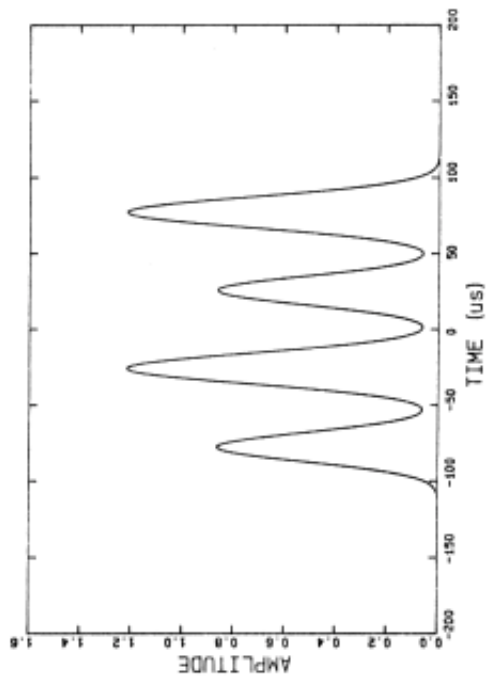


Fig. 2 Arrangement of the series of four retroreflectors which generate the aircraft type identification code. As the SLASS beam interrogates the sequence the return beam is modulated in amplitude to form a two level data word.

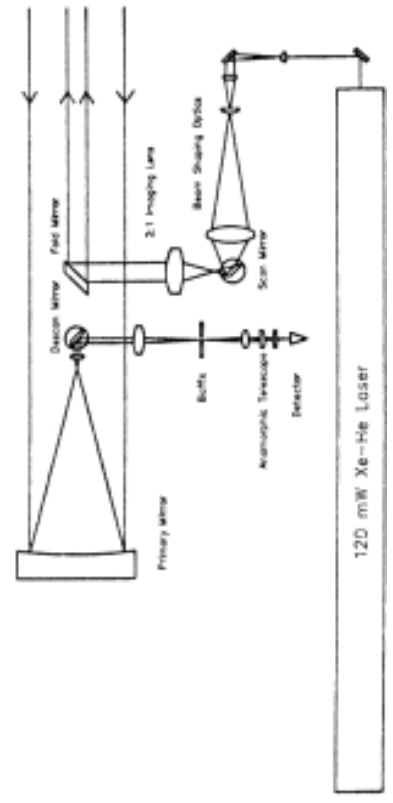


Fig. 4 The laser beam is shaped with a telescope and cylindrical lens to focus in the direction of the scan and expand in the perpendicular direction. The scan mirror is imaged onto a fold mirror at the exit aperture. The return beam is collected by the primary mirror of a telescope. After the descan mirror converts the angular motion of the return beam to lateral motion, a lens focuses the beam through a baffle which limits the FOV of the detector to the region illuminated by the laser. An anamorphic telescope squares the beam and directs it to a detector.

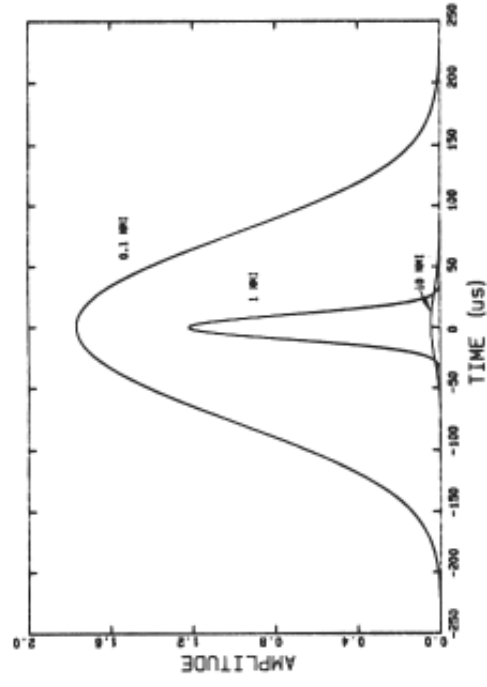


Fig. 5 Temporal dependence of the return pulses for the azimuthal scan at ranges of) 1, 1, and 10 nmi. At long range, the pulse width increases because the beam waist increases faster than the range.

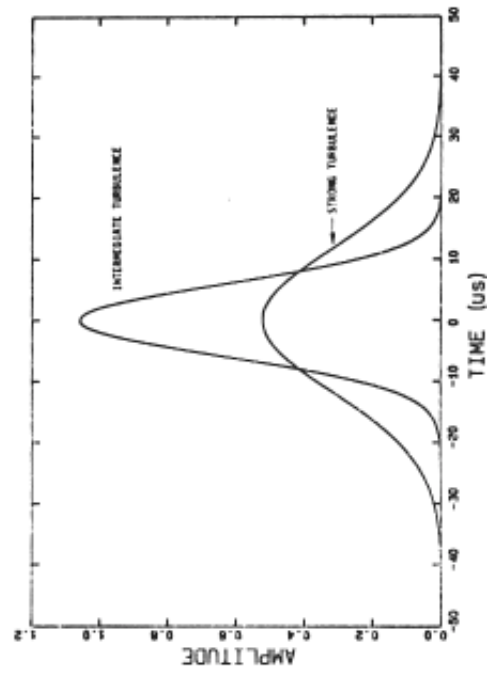


Fig. 6 Comparison of the return pulses for the azimuthal scan at a range of 2 nmi with strong and intermediate turbulence levels. The beam spread due to turbulence causes the return beam to spread in time and the peak intensity to decrease.

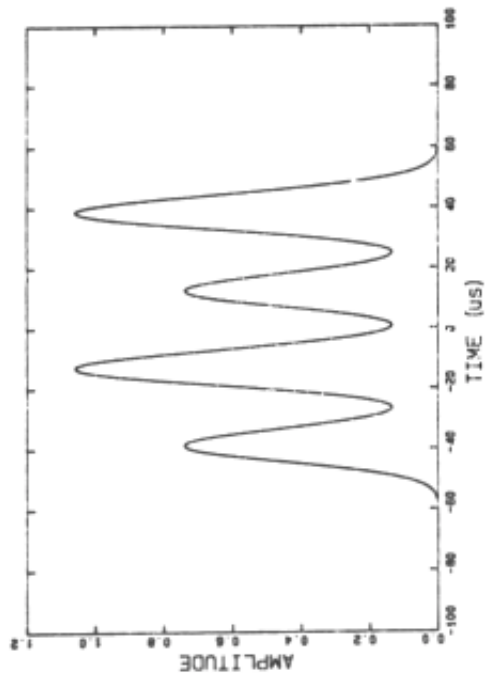


Fig. 7 Temporal dependence of the return pulse for the aircraft type identification sequence of four retroreflectors at a range of 2 nmi and with intermediate turbulence. The retroreflectors have a size of 75 mm and a 0.25 m spacing.

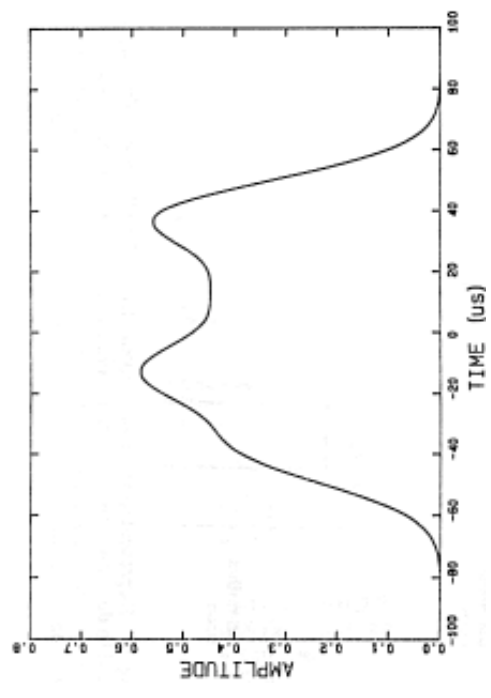


Fig. 8 Temporal dependence of the return pulse for the aircraft type identification sequence of four retroreflectors at a range of 2 nmi and with strong turbulence. The retroreflectors have a size of 75mm and a 0.25 m spacing. under these conditions, the sequence is just resolvable.

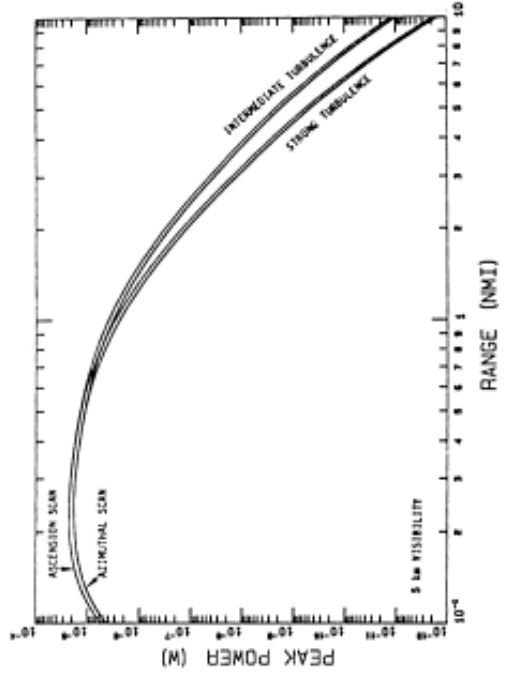


Fig. 11 The peak power in the return pulse as a function of range.

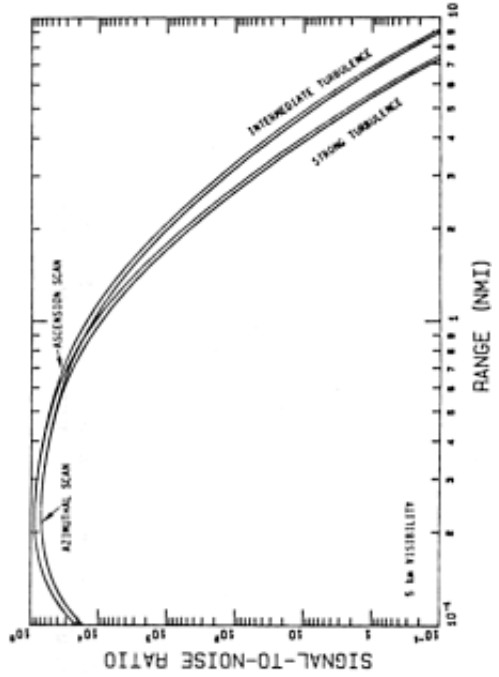


Fig. 12 SNR with 5 km visibility.

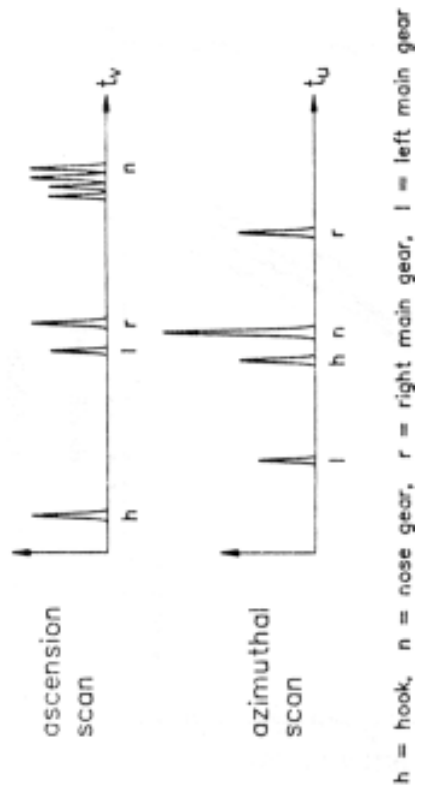


Fig. 9 Schematic representation of the return signals for the SLASS. There are two different sizes of retroreflectors. The smaller sizes are on the left main gear and are also used in the aircraft type identification sequence on the nose gear.

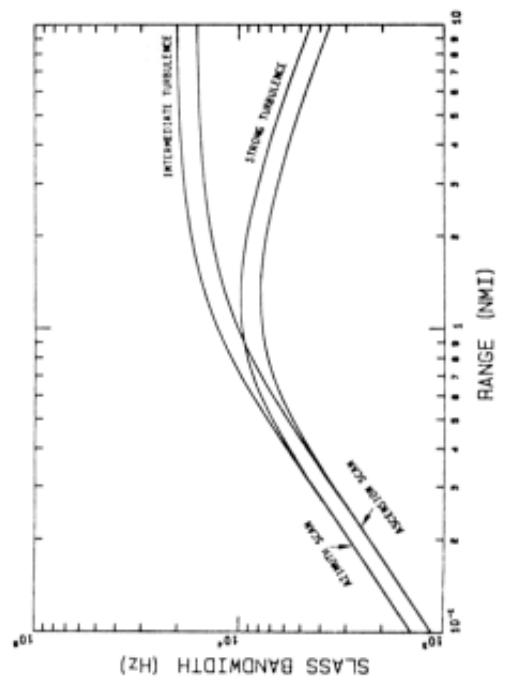


Fig. 10 Bandwidth of the SLASS signals for both strong and intermediate turbulence. The azimuthal scan has a higher bandwidth as it scans 5deg in the same time that the ascension scan covers 4 deg.

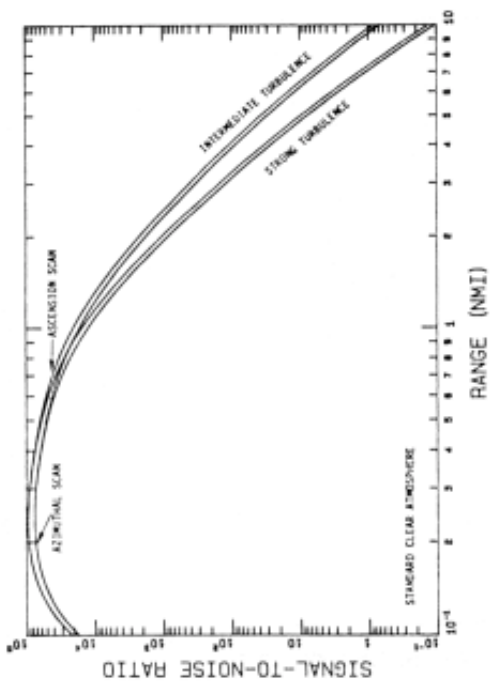


Fig. 13 SNR with 23.5 km visibility.

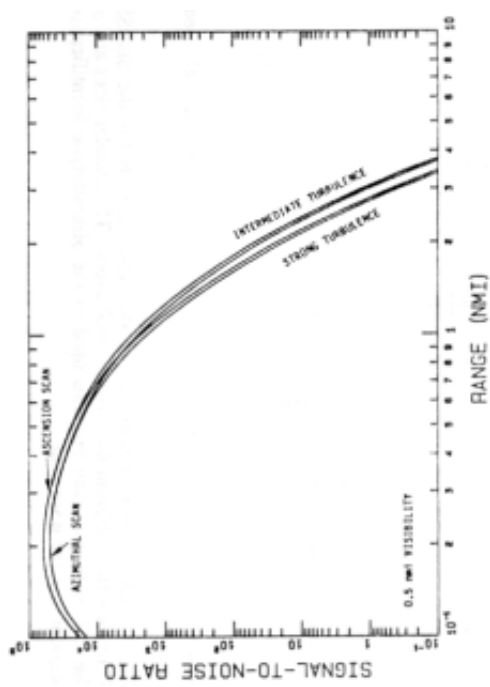


Fig. 14 SNR with 0.5 nmi visibility.

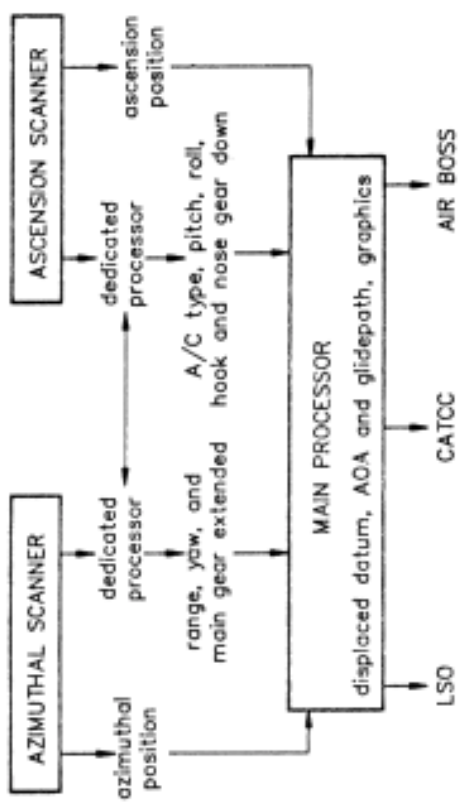


Fig. 15 Function diagram of the SLASS signal processing from data acquisition by the two scanners to displays at three stations.